INTERNATIONAL JOURNAL FOR NUMERICAL METHODS IN FLUIDS, VOL. 4, 499–509 (1984)

NUMERICAL COMPUTATIONS OF CRITICAL FLOW OVER A WEIR

M. J. O'CARROLL AND E. F. TORO

Department of Mathematics and Statistics, Teesside Polytechnic, Middlesbrough TS1 3BA, Cleveland, England

SUMMARY

Computing critical flows in hydraulics involves three problems in one: the internal flow problem, the location of the free surface and the determination of the critical flow rate. The subject can involve such difficulties as non-uniqueness, non-existence, ill-conditioning and catastrophes.

This paper discusses the difficulties relating to computing critical flows over weirs. A new rapidly convergent method of determining the critical flow rate is presented and various results are shown using it with finite element discretization and with a new streamline shifting method. Numerical results are in good agreement with published data, both numerical and experimental.

KEY WORDS Critical Flow Rate Finite Elements Free Surface Weir

INTRODUCTION

The computation of steady ideal flows with free surfaces under gravity has been the subject of a number of recent investigations, both for configurations of practical engineering interest and for fundamental enquiries on wave phenomena. The non-linear free surface problems may have non-unique solutions in certain cases. If a flow rate is prescribed too high, or if the flow domain is truncated wrongly relative to an unknown wave, there may be no solution at all. When the problem involves determining a critical flow rate, it may become ill-conditioned or catastrophic.[1]

Numerical solutions go back to the finite difference work of Southwell and Vaisey.[2] More recently finite elements[3,4] have been used to improve the representation of irregular geometry. Still more recently boundary elements have been used[5] for wave studies. The difficulties inherent in the discharge problems have been treated by *ad hoc* methods which may be uncertain or expensive for nearly critical flows. The numerical computations require the simultaneous solution of three coupled problems, namely (i) the determination of the internal velocity distribution (the ψ-problem), (ii) the location of the free surface (the H-problem), and (iii) the computation of the correct value of the discharge Q (the Q-problem).

Aitchison[4] computed critical flow over a sharp crested weir for three different triangular weir cases. By using a variational formulation in terms of stream function, the H and ψ problems are solved simultaneously. The solution to the Q-problem is found from an interpolation procedure based on the reversal of phase of upstream waves as Q increases through the critical value. All computations are carried out on channels with long upstream

0271–2091/84/060499–11$01.10

Received 14 December 1982
Revised 17 March 1983

and downstream sections. The computational flow domain is then large, which results in a correspondingly large computational effort. Moreover, these upstream and downstream sections are not of great interest, since the solution is expected to be asymptotically uniform there. By using a different technique of finding critical Q, it is possible to take a much shorter computational region.[6] An added computational cost in Aitchison's work arises from numerical computation of derivatives of the functional.

A variational approach to computing the critical flow rate was introduced by Varoglu and Finn.[7] They modified a functional depending on stream function and made it stationary with respect to flow rate as well as with respect to stream function. However, the extra condition obtained is only a combination of the flow equations and the free-surface pressure condition. It introduces no criterion which can fix the flow rate. The iterative method converges to a plausible result, but the dependent set of stationary equations could admit a range of flow rates, so the method is not valid for determining critical flows.

Historically the variational method for stream function was incorrectly adapted from that for velocity potential. Luke[8] gave the velocity potential principle but then Ikegawa and Washizu[3] expressed the same functional in terms of stream function instead of using the complementary principle. O'Carroll and Harrison[9] formulated a correct principle for the stream function giving the free surface conditions naturally under the constraint of constant stream function on the surface. This has been used successfully by other authors. A fuller explanation appears in reference 10.

In this paper we report on numerical computations of critical flow over a weir using three different algorithms developed by the authors.[6] All computations are carried out in short flow domains, which results in considerable savings. The solution to the Q-problem is based on the observation that for a range of values of the discharge Q, the upstream displacement of the computed surface from the appropriate asymptotic level varies almost linearly with Q^2, and this displacement is zero for the critical solution. This results in a rapidly convergent iteration procedure.

Numerical results for three weir cases are in good agreement with those published by Aitchison[4] as well as with published experimental data.[11]

STATEMENT OF THE PROBLEM

We consider a two-dimensional flow domain R as illustrated in Figure 1. The stagnation level is measured by H_0, the channel length by L, the bed profile (BE) by $y = b(x)$ and the

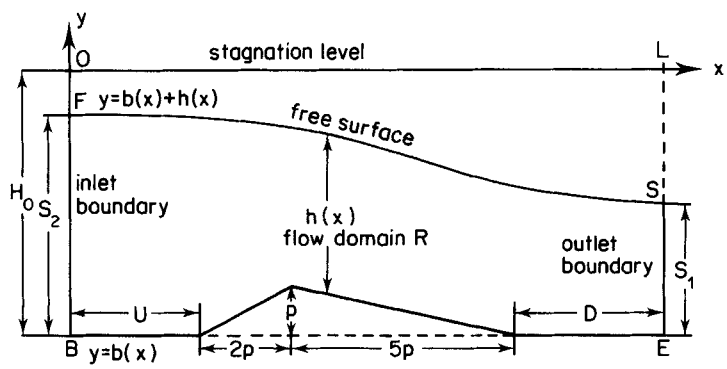

Figure 1. Flow domain

free surface position (FS) by $y = b(x) + h(x)$. Here $h(x)$ measures the depth of flow and is to be determined, whereas $b(x)$ is prescribed and in this case it is determined by a triangular weir placed on a horizontal bottom. The weir height at the crest is p and the other dimensions are as indicated there. The inlet boundary BF and the outlet boundary ES are placed at distances U and D, respectively, from the weir ends.

The free surface FS is under the influence of gravity, and effects of surface tension are neglected. Considering the flow in terms of a stream function ψ, and assuming that the flow is steady, incompressible, non-viscous and irrotational, the stream function satisfies Laplace's equation in R. As regards the boundaries BF and ES, a condition of normal flow is imposed by requiring the vanishing of the normal derivative $\partial\psi/\partial n$. This condition corresponds to asymptotically uniform flows upstream and downstream provided U and D are large enough. The bed and free surface are streamlines. For an assumed total head H_0, a discharge Q and a free surface position, the ψ-problem is governed by the following boundary value problem:

$$\begin{aligned} &\partial^2\psi/\partial x^2 + \partial^2\psi/\partial y^2 = 0 \text{ in } R \\ &\psi = Q \text{ on BE} \quad \text{and} \quad \psi = 0 \text{ on FS} \\ &\partial\psi/\partial n = 0 \text{ on BF and ES} \end{aligned} \tag{1}$$

The solution of (1) gives the velocity distribution $\mathbf{V}$ in R with $\mathbf{V}$ defined as $\mathbf{V} = (-\partial\psi/\partial y, \partial\psi/\partial x)$.

An additional boundary condition on FS is to be satisfied. The pressure is prescribed there and taken as atmospheric. Bernoulli's law then gives

$$\tfrac{1}{2}(\partial\psi/\partial n)^2 + gy = 0 \text{ on FS} \tag{2}$$

where g is the acceleration due to gravity. This equation provides a necessary condition for finding the position of the free surface (the H-problem).

The free boundary value problem (1)–(2), which governs the combined H–ψ problems, is equivalent to the variational problem[9] with non-dimensionalized functional

$$J(h(x), \psi(x, y)) = \int_0^L \int_{b(x)}^{b(x)+h(x)} \{\tfrac{1}{2}(\nabla\psi)^2 - y\}\, dx\, dy \tag{3}$$

and the constraints

$$\psi = Q \text{ on BE} \quad \text{and} \quad \psi = 0 \text{ on FS} \tag{4}$$

This means that for a given stagnation level and discharge Q (within a certain range of values for Q) a stationary point of J is a solution to the combined H–ψ problems.

In (3) and (4) all quantities have been non-dimensionalized with respect to length H_0 (see Figure 1) and time $(H_0/g)^{1/2}$, including the x and y co-ordinates.

It is worth noting that the mathematical formulation of the H–ψ problem is valid for any bed configuration. Thus, the derived numerical methods being used to compute critical flows over a weir can also be applied to solve problems having other bed profiles.[6]

When considering the special case of uniform and horizontal flows, the governing stationary equations are reduced to the purely algebraic relation

$$2h^3 - 2h^2 + Q^2 = 0 \tag{5}$$

This cubic equation has two physically meaningful solutions, S_1 and S_2, in the real interval $(0, 1)$ for a prescribed value of the discharge Q in $(0, (8/27)^{1/2})$. For $Q^2 = 8/27$, S_1 and S_2 coalesce and $S_1 = S_2 = 2/3$. S_1 and S_2 represent rapid and tranquil horizontal uniform flows,

respectively. Transition from S_2 to S_1 is made possible by constrictions such as sluicegates, spillways, weirs and other control mechanisms. In this context we use the term critical flow for a smooth transitional flow with asymptotic depth S_2 upstream and asymptotic depth S_1 downstream (see Figure 1).

Here we deal with computations of critical flow over a weir. This involves the simultaneous solution to the Q–H–ψ problem, that is to say, we need to compute the correct value of the discharge Q_c, the correct position of the associated free surface and the flow distribution in the corresponding domain. We consider four weir cases A, B, C and D with dimensions as illustrated in Table I. For the examples A, B and C there are numerical results computed by Aitchison,[4] with which we make comparisons. In addition, comparisons are also made with experimental data obtained from British Standards.[11]

In the numerical computation of the H–ψ problem we use our algorithms FETR, FEBI and NODE, which are based on the stream function variational formulation of the problem.

The algorithms FETR and FEBI are derived from a semiregular finite element discretization of the flow domain. The former assumes linear interpolation for ψ on each triangular element and the latter assumes a bilinear interpolation on quadrilateral elements. FEBI requires an isoparametric transformation of the flow domain. By performing exact integration and differentiation, the H–ψ problems are then governed by explicit sets of non-linear algebraic equations (for the H-problem) and linear algebraic equations (for the ψ-problem). Numerical solution to the combined H–ψ problem (when Q is prescribed) is then obtained by alternately solving the non-linear and linear systems of equations. The third algorithm (NODE) is obtained by using a Ritz–Kantorovich type of approximation for ψ in the y-direction in which the problem remains continuous in the x-direction. The stationary conditions yield a system of non-linear ordinary differential equations in x for the streamlines. A finite difference discretization in the x-direction then produces an explicit system of non-linear algebraic equations. This system governs both the H and ψ problems and thus there is no alternating procedure between two systems (as with FETR and FEBI). Full details, comparisons and discussion of these algorithms are given by Toro.[6]

FLOW DOMAIN AND COMPUTATIONAL STRATEGY

The flow domain (Figure 1) is completely determined by the bed profile, the position of the inlet and outlet boundaries and the position of the free surface, which is to be computed. The bed profile is prescribed and is given by the dimensions of the particular weir being considered. Also, the position of the end boundaries BF and ES is prescribed, but care is required when choosing the distances U and D since the boundary conditions impose normal flow. Clearly, when these boundaries are too close to the weir ends, the imposed boundary conditions are not satisfied by the critical flow. As a result the computations (for a prescribed value of the discharge Q) fail to find a solution. The asymptotic level S_1 downstream of the weir can only be attained exactly when the length D is infinite. But, owing to the discretization of the problem, the boundary conditions at ES can be approximately satisfied for a relatively short distance D. As regards the satisfaction of the boundary conditions at BF, the situation is different, since the choice of a finite distance U can correspond to a solution of the continuous problem with upstream waves. Moreover, in the critical flow the asymptotic level S_2 upstream is attained at a short distance U, depending obviously on the weir height. This observation is based on our computations and the solution profiles of Aitchison.[4] In the computations, it is therefore justified to use a short channel and our

numerical results support this argument. This results in appreciable savings in computational effort.

The dimensions for the four weir examples considered in this paper are given in Table I. For the examples A, B and C Aitchison[4] used the same values of the ratio H_0/p, but much larger values of U/p and D/p.

Table I. Definition of computational flow domain of four weir cases

Case	H_0/p	U/p	D/p
A	7·90	7	7
B	5·69	4	4
C	4·63	2	4
D	5·00	2	3·5

Our process starts by prescribing a value Q_1 of the discharge, then solving the H–ψ problems to obtain a surface profile $\mathbf{H}_1$ and a corresponding velocity distribution in the interior of the domain. Here $\mathbf{H}_1$ is a vector given as $\mathbf{H}_1=(h_1^1, h_2^1, \ldots, h_m^1)$, where h_k^1 represents the depth of flow at station k. Normally, the computed profile determined by $\mathbf{H}_1$ is not the required free surface and has a displacement $d_1=h_1^1-S_2^1$ at the inlet boundary BF, where S_2^1 is the tranquil one-dimensional solution corresponding to Q_1 and computed from equation (5).

In a similar way a second prescribed discharge Q_2 gives rise to a surface profile determined by $\mathbf{H}_2=(h_1^2, h_2^2, \ldots, h_m^2)$ with a corresponding internal velocity distribution. Now the displacement at BF is $d_2=h_1^2-S_2^2$ where S_2^2 is the tranquil solution corresponding to Q_2, computed from equation (5).

In Figure 2 we show two computed surface profiles $\mathbf{H}_1$ and $\mathbf{H}_2$ for case D of Table I with $Q^2=0{\cdot}20$ and $Q^2=0{\cdot}22$. The computations were carried out using the NODE algorithm, which provides automatically the internal streamlines, also displayed there. The mesh used has 26 stations and 5 streamlines (26×5).

In order to observe the behaviour of the surface profile at the inlet when Q is varied we carried out many computations. In Table II we show prescribed values Q_i^2 and the displacements d_i of the corresponding computed surface profiles $\mathbf{H}_i$.

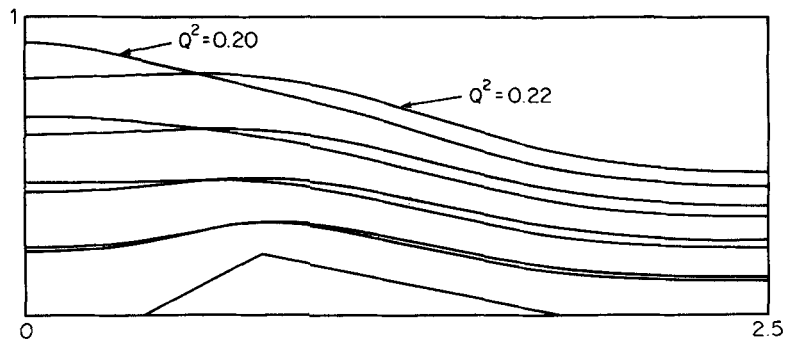

Figure 2. Computed free surfaces and streamline profiles for $Q^2=0{\cdot}20$ and $Q^2=0{\cdot}22$ using NODE algorithm

Table II. Displacement values (d_i) of computed surface profiles for prescribed values Q_i^2

	P_1	P_2	P_3
Q_i^2	0·20	0·21	0·22
d_i	0·0485	0·0007	−0·0478

By observing Table II and Figure 2 we clearly see that the required solution Q_c^2 with a corresponding zero displacement d lies between $Q^2 = 0{\cdot}20$ and $Q^2 = 0{\cdot}22$, and the point $P_2 = (0{\cdot}21, 0{\cdot}0007)$ is very close to the solution. The empirical results of the British Standard[11] give $Q^2 = 0{\cdot}2006$ for this weir, but it is to be expected that the computed ideal flow admits a slightly larger discharge.

In all computations we observe that the $Q^2 - d$ relation behaves almost linearly (see Table II). Thus we implemented an iterative procedure for computing the critical value Q_c based on linear interpolation:

$$Q_i^2 = Q_{i-2}^2 - d_{i-2}(Q_{i-1}^2 - Q_{i-2}^2)/(d_{i-1} - d_{i-2}) \tag{6}$$

Once the surface profile $\mathbf{H}_i$ (and the internal velocity distribution) corresponding to Q_i has been computed we test whether the displacement at the inlet satisfies

$$d_i = |h_1^i - S_2^i| < \text{TOLD} \tag{7}$$

where TOLD is a preassigned small non-negative number. In the present computations we took $\text{TOLD} = 10^{-4}$. If at any stage, including of course the two initial steps, relation (7) is satisfied we stop the interation procedure. The algorithm for computing Q_c is described by the flow chart of Figure 3.

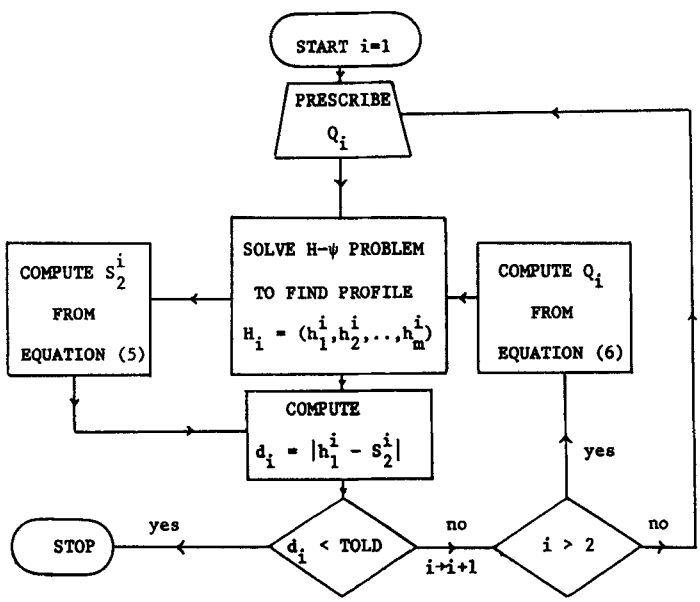

Figure 3. Algorithm for computing Q_c

In the computations reported here, it took normally two iterations, after the two initial values, to obtain the solution Q_c to the critical discharge problem. In the algorithm (Figure 3) the initial values Q_1 and Q_2 may be taken to lie anywhere in the interval $(0, \sqrt{(8/27)})$, but it is obviously more realistic to choose them to be greater than the experimental result.

It may happen that no solution $\mathbf{H}_i$ is computed for a given Q_i. This could be particularly the case for the first two guessed values Q_1 and Q_2. Such a situation is an indication that the inlet boundary BF is misplaced. That is to say, the given value for the discharge has an associated surface profile with corrugations upstream of the weir for which the position of BF does not approximately coincide with a crest or trough. The imposed boundary conditions then do not correspond to an existing solution. This difficulty can be effectively overcome by trying a new position for BF or a new value for Q.

NUMERICAL RESULTS

In this section we report on the computed solution to the complete Q–H–ψ problem for the three weir cases A, B and C of Table I. The computation of the H–ψ problem in each case is carried out by using the algorithms FETR, FEBI and NODE with meshes 22×4 (for case A), 16×4 (for case B) and 14×4 (for case C).

In Table III we show the complete Q-iteration process (Figure 3) in the computations for cases A, B and C using FETR to solve the H-ψ problem. In all three examples four Q-computations were carried out and only two steps in the iteration process were necessary to find the solution.

Table III. Q-iteration process for cases A, B and C in FETR computations

	Case A		Case B		Case C	
	Q_i^2	d_i	Q_i^2	d_i	Q_i^2	d_i
1	0·50990	−0·0054	0·46840	0·0553	0·43451	0·0565
2	0·51186	−0·0195	0·47980	−0·0122	0·45166	−0·0251
3	0·50916	−0·0002	0·47776	−0·0003	0·44643	−0·0017
4	0·50912	0.0000	0·47770	0·0000	0·44608	0·0000

When solving the H–ψ problem for a given Q using the finite element algorithms FETR and FEBI, the alternating iteration process between the H and the ψ problems is a potential source of difficulty. The NODE algorithm however, is very well behaved. In Table 4 we show the number of H–ψ iterations for all three cases A, B and C when using FETR.

Table IV. Number of H–ψ iterations in FETR computations

	Cases		
Q-iteration	A	B	C
1	8	17	19
2	7	12	12
3	8	9	10
4	3	4	6

Generally, the number of H–ψ iterations in the finite element computations (FETR and FEBI) decreases as the critical solution is approached. This is partly due to the way in which we have chosen the required initial profile for the solution of the H–ψ problem at each Q-iteration. For $i>2$ we take as initial profile in the H–ψ problem the computed profile at stage $i-1$. For the first two cases we normally chose guessed profiles that take on the level S_2 upstream and S_1 downstream with an estimated smooth transition around the weir.

Complete numerical results for critical discharge are shown in Table V, where, for comparison, we have also included the numerical results due to Aitchison[4] and the experimental results from the British Standard.[11]

Table V. Computed values for critical discharge for cases A, B and C using algorithms FETR, FEBI and NODE

	Case	A	B	C
	H_0/p	7·90	5·69	4·63
Present computations	FETR	0·5091	0·4777	0·4461
	FEBI	0·5101	0·4796	0·4493
	NODE	0·5102	0·4791	0·4477
Aitchison		0·5110	0·4798	0·4517
Experimental		0·5110	0·4684	0·4346

The slight difference between our computed values of the critical discharge and those of Aitchison is due to slightly different discretization. Aitchison has a much larger computational flow domain, especially upstream of the weir. Also, Aitchison's mesh has one more node in the y-direction and has special mesh refinement near the crest of the weir.

Both Aitchison's and the present results are a continuous ideal flow model which can admit neither a boundary layer nor a circulation bubble behind the crest, as occur in real flow. Such limitations account for the small discrepancy between numerical and experimental results, which increases with relative weir size.

Solution surface profiles for cases A, B and C using the FETR and NODE algorithms are shown in Figures 4, 5 and 6, respectively.

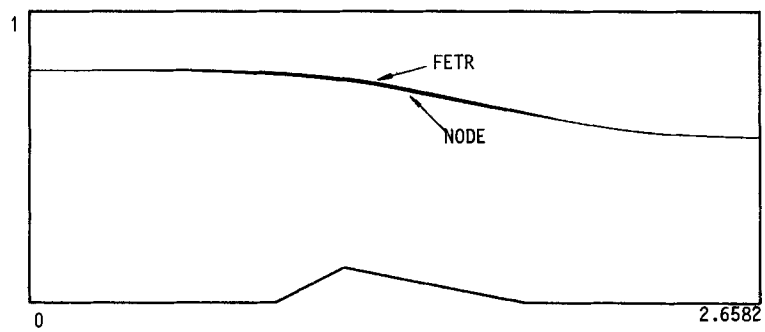

Figure 4. Computed critical free surface profiles for case A by FETR and NODE algorithms

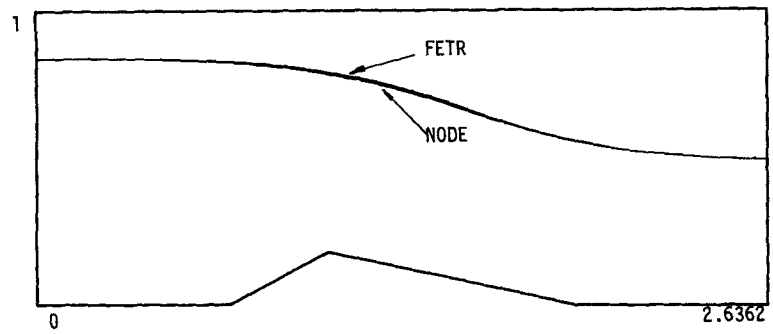

Figure 5. Computed critical free surface profiles for case B by FETR and NODE algorithms

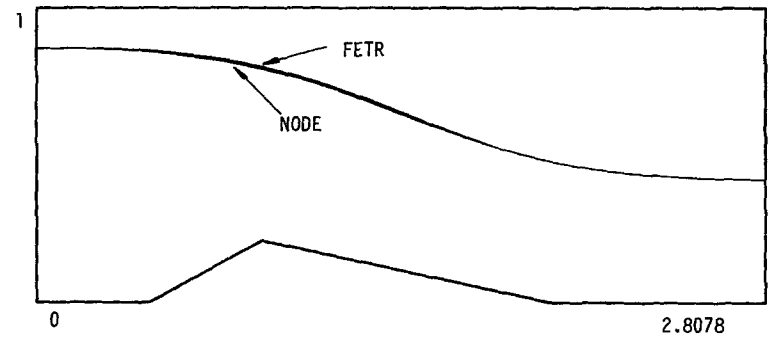

Figure 6. Computed critical free surface profiles for case C by FETR and NODE algorithms

MESH REFINEMENTS AND DOMAIN EXTENSIONS

In this section further computations are given for the weir case B to show the effect of enlarging both the upstream and downstream sections and refining the mesh in various ways. In Table VI we show the various B-subcases and the computed values for the critical discharge Q_c

Table VI. Computed values of Q_c for various channel lengths and meshes

Case	U	D	Mesh	Present computations FETR	Present computations NODE	Aitchison's result
B	$4p$	$4p$	16×4	0·47770	0·47906	
BA1	$13p$	$10p$	31×4	0·47868	0·47986	
BA2	$13p$	$10p$	31×5	0·47861	0·47966	0·4798
B1	$4p$	$4p$	16×8	0·47766	0·47904	
B2	$4p$	$4p$	31×4	0·47869	0·47934	
B3	$4p$	$4p$	31×8	0·47852	—	

Cases BA1 and BA2 of Table VI have long upstream and downstream sections, and the results show the justification of using a short channel. Both BA1 and BA2 correspond to Aitchison's flow geometry for weir B ($H_0/p = 5{\cdot}69$, Table I). Meshes are still different with BA2 being the closest case to that of Aitchison (31×5). The results indicate that a longer channel brings about an increase in the value of Q_c. Compare value Q_c of case B to those of BA1 and BA2 under FETR, for instance. The increase is about 0·2 percent. The increase observed on the NODE computations is even smaller.

The small difference observed between cases BA1 and BA2 suggests that a mesh refinement in the y-direction alone results in a slight decrease in the computed value of Q_c. This is found to be the case in other computations as well, although it is somewhat surprising since more degrees of freedom in the discretization might be expected to lead to a higher discharge. The effect may be due to discretization arising from elongation of element shape.

Refinement in the x-direction alone results in an increased value for Q_c. This is clearly seen in Table VI. Simultaneous refinements in both x and y directions bring about an increased value for Q_c. In this case, halving the mesh size in both directions increases the computed Q_c by less than about 0·2 per cent.

As regards the computed free surface profiles shown in Figures 4–6, a difference between FETR and NODE computed results can be observed in the vicinity of the weir. This becomes more noticeable as the weir height increases. In Table VII we show the height h_c of the computed free surface at the crest of the weir, for different cases.

Table VII. Height h_c of computed free surface profiles at weir crest

Case	B	BA1	BA2	B3
FETR	0·7863	0·7862	0·7848	0·7803
NODE	0·7802	0·7802	0·7808	—

The enlargement of the computational flow domain produces almost no variation in the computed value for h_c. More appreciable but still small variations occur with mesh refinements. More importantly, the value of h_c in the FETR computations becomes closer to that of the NODE computations under mesh refinement in both the x and y directions, confirming that the difference in the two algorithms is due to discretization.

CONCLUDING REMARKS

A rapidly convergent iterative procedure for computing the correct value Q_c for the initially unknown critical discharge in flows over a weir has been presented. The method requires only short computational flow domains with consequent savings in computation.

At each Q-iteration, the solution of the non-linear problem of finding the free surface position (and the corresponding internal velocity distribution) is efficiently computed by three different algorithms developed by the authors. These algorithms can also be applied to solve open channel flow problems with arbitrary bed profile.

Application of the method for computing critical flow to a family of weirs yields numerical results that are in good agreement with published data, both numerical and experimental.

REFERENCES

1. M. J. O'Carroll, 'Fold and cusp catastrophies for critical flow in hydraulics', *Appl. Math. Modelling*, **1,** 108–109 (1976).
2. R. V. Southwell and G. Vaisey, 'Relaxation methods applied to engineering problems XII. Fluid motions characterised by free streamlines', *Phil. Trans. Roy. Soc.*, **A240,** 117–161 (1946).
3. M. Ikegawa and K. Washizu, 'Finite element method applied to analysis of flow over a spillway crest', *Int. J. Num. Meth. Eng.*, **6,** 179–189 (1973).
4. J. M. Aitchison, 'A finite element solution for critical flow over a weir', *Proc. 3rd International Conference on Finite Elements in Flow Problems*, Banff, Alberta, Canada, 1980.
5. P. L. Betts and T. T. Mohamed, 'Water waves: a time-varying unlinearised boundary element approach', *Proc. 4th Int. Symp. Finite Element Methods in Flow Problems*, University of Tokyo Press, 1982, pp 923–929.
6. E. F. Toro, 'Finite element computation of free surface problems', *Ph.D. Thesis*, Mathematics Department, Teeside Polytechnic, Middlesbrough, Cleveland, England, 1982.
7. E. Varoglu and W. D. L. Finn, 'Variable domain finite element analysis of free surface gravity flow, *Computers and Fluids*, **6,** 103–114 (1978).
8. J. C. Luke, 'A variational principle for a fluid with a free surface', *J. Fluid Mech.*, **27,** 395–397 (1967).
9. M. J. O'Carroll and H. T. Harrison, 'Variational techniques for free strealine problems', *Proc. 2nd Int. Symp. Finite Elements in Flow Problems*, Genoa, 1976, pp 485–495.
10. M. J. O'Carroll, 'A variational principle for ideal flow over a spillway', *Int. J. Num. Meth. Eng.*, **15,** 767–789 (1980).
11. British Standards, *BS* 3680, *Part 4B*, 1969.